RAPID COMMUNICATIONS

PHYSICAL REVIEW B VOLUME 52, NUMBER 8 15 AUGUST 1995-II

# Density-matrix renormalization-group calculation of correlation functions in the one-dimensional Hubbard model

Shaojin Qin
*Institute of Theoretical Physics, Academia Sinica, P.O. Box 2735, Beijing 100080, China*

Shoudan Liang
*Department of Physics, Pennsylvania State University, University Park, Pennsylvania 16802*

Zhaobin Su
*Institute of Theoretical Physics, Academia Sinica, P.O. Box 2735, Beijing 100080, China*

Lu Yu
*International Centre for Theoretical Physics, P.O. Box 586, 34100 Trieste, Italy*
*and Institute of Theoretical Physics, Academia Sinica, P.O. Box 2735, Beijing 100080, China*
(Received 22 May 1995)

We have studied correlation functions of the one-dimensional Hubbard model using the density-matrix numerical renormalization-group approach. The singularity exponents of the momentum distribution at $k=k_F$ and $3k_F$, as well as the power-law singularity of the spin-correlation function, are computed for large $U$ ($U/t=10^3$). The momentum-distribution exponent at $k=k_F$ and the spin-correlation exponent are in agreement with the analytic results, while the calculated exponent for momentum distribution at $k=3k_F$ is about $\frac{3}{4}$, which disagrees with the analytically predicted value $\frac{9}{8}$. We also discuss several techniques for an accurate calculation of the correlation functions.

Ever since the discovery of high-$T_c$ superconductors and the realization that electron-electron correlations play an important role in these materials, the Hubbard model has attracted a great deal of attention. Following a suggestion by Anderson that the one-dimensional (1D) Hubbard model serves as a paradigm for the two-dimensional system,[1] a number of techniques has been used to study the 1D Hubbard model, which has a non-Fermi liquid ground state. The spin- and charge-correlation functions show power singularities at zero temperature. Also, the Fermi distribution function does not have a finite jump, but rather a power-law singularity at the Fermi surface. Using the large $U$ limit of the Bethe ansatz solution of the Hubbard model,[2] Ogata and Shiba[3] pioneered an explicit numerical calculation of the singularity exponents for various correlation functions. Soon afterwards, the exponent of the spin-correlation function was calculated analytically,[4] and all the exponents were derived by the bosonization technique[5] and mapping onto a conformal field theory (CFT),[6] based on the Bethe ansatz solution[2] and the Luttinger liquid framework, proposed by Haldane.[7] These exponents have also been reproduced by a "mean-field-type" calculation using non-Abelian gauge transformations.[8] In particular, for the large $U$ limit, an exponent of 1/8 for the momentum distribution function at $k_F$ was predicted which has been verified at the same time by numerical calculations.[3,9] A power of 9/8 at large $U$ has also been predicted to show up at $k=3k_F$. However, there is, so far, no strong numerical evidence to support it.[10]

In this paper we use the recently developed, powerful density-matrix renormalization-group (DMRG) method[11] to calculate the correlation functions for the large $U$ Hubbard chains for system length up to 24 sites with periodic boundary conditions. The key idea behind DMRG is to keep the most significant states of the block density matrix instead of eigenstates of the block Hamiltonian. The method has been tremendously successful in studying the spin-1 Heisenberg chain[12,13] and the Kondo lattice problem.[14] We have calculated the singularity exponents of the momentum-distribution function at $k_F$ and $3k_F$ as well as the power-law spin-spin correlation function at $2k_F$. Our result for the singularity at $k_F$ is in agreement with the evaluation by Ogata and Shiba[3] from the exact solution. Our exponent for the spin-spin correlation function at $2k_F$ also agrees with the analytical results. However, the exponent for the momentum-distribution function that we obtained at $3k_F$ is about 3/4, which is smaller than 9/8, expected from the scaling relations.[3–6,15] This poses new questions for further study near this singularity.

We study the correlation functions for the 1D Hubbard model,

$$H=-t\sum_{i\sigma}(c^{\dagger}_{i\sigma}c_{i+1\sigma}+\text{H.c.})+U\sum_{i}n_{i\uparrow}n_{i\downarrow}, \qquad (1)$$

where $c^{\dagger}_{i\sigma}$ creates an electron of spin $\sigma$ at site $i$. We study the system at 1/4 filling with a total number of electrons $N=N_{\uparrow}+N_{\downarrow}$ and $N_{\uparrow}=N_{\downarrow}=L/4$, $U/t=10^3$. We use periodic boundary condition (PBC) for $L=4,12,20$ and antiperiodic boundary condition for $L=8,16,24$, following the reasoning of Ogata and Shiba.[3] The momentum distribution and spin correlation are evaluated explicitly as

 

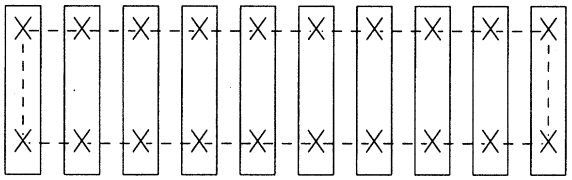

FIG. 1. The 1D array of cells used in our DMRG calculations on Hubbard chains. Sites are indicated by ×. The dashed lines represent the electron hoppings. The boxes are the inserted cells.

$$n(k)=\frac{1}{L}\sum_{i,j}\langle c_{i\uparrow}^{\dagger}c_{j\uparrow}\rangle e^{ik(i-j)},$$

$$S(k)=\frac{1}{L}\sum_{i,j}\langle s_i^z s_j^z\rangle e^{ik(i-j)}, \tag{2}$$

where $s_i^z=(n_{i\uparrow}-n_{i\downarrow})/2$ and $\langle\ \rangle$ denotes the ground state expectation value. We use the infinite chain DMRG method to prepare the initial blocks, and then use the finite chain method to calculate the correlation functions. In order to treat PBC, we use a configuration somewhat different from the conventional one. The Hubbard chain is represented by an array of cells with two sites in each cell (see Fig. 1), where the line between the sites (symbol ×) indicates the electron hopping. The two edge cells differ from the rest by having electron hopping between the two sites within the cell. We insert two cells (i.e., four sites) in the middle of the array at each step. Although this makes the working Hilbert space larger and calculation more difficult, inserting four sites is commensurate with 1/4 filling we study and makes the calculation converge much faster, as discussed below.

We first report the results of the calculated correlation functions before turning at the end of the paper, to a discussion of techniques that make these calculations possible. Our calculations are done for chain length $L=4,8,12,16,20,24$ and by keeping up to 100 optimized states at each step in both infinite chain initialization and the finite chain iterations. The truncation error is less than $10^{-4}$ at all steps. One complete finite chain iteration involves optimizing each of the block state sets from a small block size to a large block size by moving the inserted cell from one edge to the other (Fig. 1). After three iterations, the change in the ground state energy is at the eight digit between the successive iterations. We use the ground state wave function to calculate $n(k)$ and $S(k)$ when the optimizing steps come to the middle of the chain in the finite chain iteration, since this step gives the lowest ground state energy and the best wave function. We accept the calculated $n(k)$ and $S(k)$ as final results when the percentage differences in $n(k)$ and $S(k)$ evaluated in successive iterations are less than $10^{-3}$. The final results are obtained usually after several runs of finite chain iterations. The relative error $10^{-3}$ is taken into account when analyzing the final results. The $n(k)$ for $L=8$ to 24 are plotted in Fig. 2, and the $S(k)$ are plotted in Fig. 3. The magnitudes of $n(k)$ and $S(k)$ around their singularities are listed in Table I. In Fig. 2, the singularities at $k=k_F$ and $k=3k_F$ of $n(k)$ are obvious. The exponent $\alpha$ of $n(k)$ at $k=k_F$ is defined as[15]

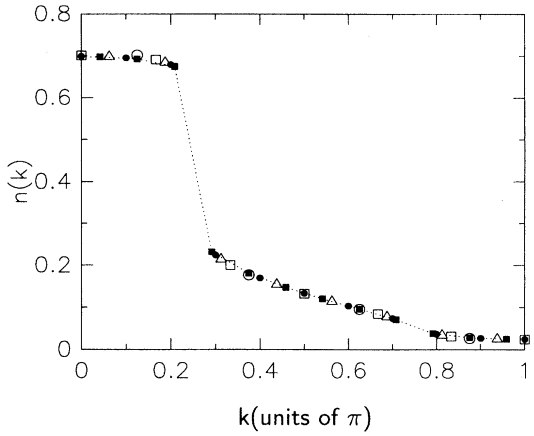


FIG. 2. The momentum-distribution function $n(k)$ for the Hubbard chain at filling $N_\uparrow/L=N_\downarrow/L=1/4$. Two singularities at $k_F=\pi/4$ and $3k_F=3\pi/4$ are evident. The open circles are for $L=8$; open squares, $L=12$; open triangles, $L=16$; round dots, $L=20$; and black squares, $L=24$. The dotted line indicates $n(k)$ for $L=24$.

$$n(k)=n_{k_F}-C|k-k_F|^{\alpha}\mathrm{sgn}(k-k_F), \tag{3}$$

where $n_{k_F}=1/2$. Following Ogata and Shiba,[3] using $n_{k_F}=1/2$, we have determined the exponent $\alpha$ by plotting in Fig. 4 $\ln[n_{k_F}-n(k)|]-\ln[|n_{k_F}-n(k_0)|]$ versus $\ln(|k-k_F|)-\ln(|k_0-k_F|)$ using one $k$ value from each $L$ that is the closest to $k_F$. $k_0$ is taken to be the one of $L=24$. We get $\alpha\sim 1/8$. Using the same method, we have

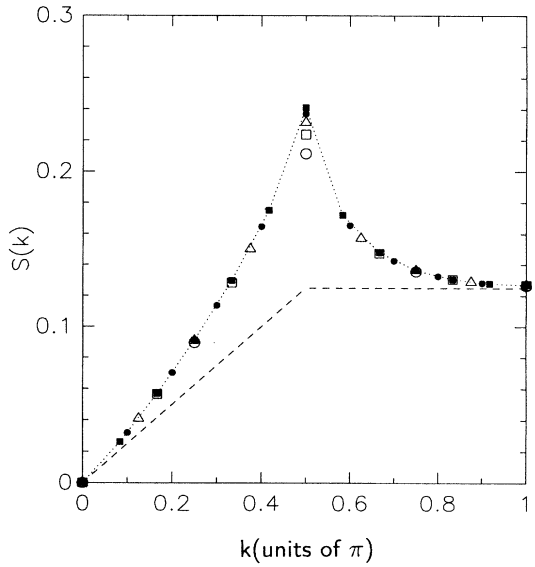


FIG. 3. The Fourier transformation $S(k)$ of the spin-spin correlation function $\langle s_i^z s_j^z\rangle$. The singularity is at $2k_F=\pi/2$, $S(0)=(\Sigma s_i^z)(\Sigma s_i^z)/L=0$, and $S(\pi)\sim 0.125$ for filling 1/4. The open circles are for $L=8$, open squares for $L=12$, open triangles for $L=16$, round dots for $L=20$, and black squares for $L=24$. The dotted line indicates $S(k)$ for $L=24$, while the dashed line is $S(k)$ for $U=0$.

TABLE I. $n(k)$ and $S(k)$ around their singularities. Filling $N_\uparrow = N_\downarrow = L/4$, on-site interaction $U/t = 10^3$.

| $L$ | 8 | 12 | 16 | 20 | 24 |
|---|---|---|---|---|---|
| $n(k_F - \pi/L)$ | 0.7014 | 0.6909 | 0.6840 | 0.6787 | 0.6744 |
| $n(k_F + \pi/L)$ | 0.1769 | 0.1999 | 0.2140 | 0.2240 | 0.2318 |
| $n(3k_F - \pi/L)$ | 0.09518 | 0.08384 | 0.07749 | 0.07337 | 0.07048 |
| $n(3k_F + \pi/L)$ | 0.02652 | 0.03085 | 0.03398 | 0.03629 | 0.03806 |
| $S(2k_F - 2\pi/L)$ | 0.08966 | 0.1284 | 0.1502 | 0.1646 | 0.1750 |
| $S(2k_F)$ | 0.2114 | 0.2237 | 0.2314 | 0.2369 | 0.2409 |
| $S(2k_F + 2\pi/L)$ | 0.1357 | 0.1473 | 0.1572 | 0.1653 | 0.1720 |

also plotted in Fig. 4 $\ln[|n_{3k_F} - n(k)|] - \ln[|n_{3k_F} - n(k_0)|]$ versus $\ln(|k - 3k_F|) - \ln(|k_0 - 3k_F|)$ for $k$, the closest to $3k_F$ for each $L$ with $k_0$ being the one of $L = 24$. $n_{3k_F} = 0.051$ is used to get the best fit. Thus we get $\beta \sim 3/4$ in $n(k) = n_{3k_F} - C|k - 3k_F|^\beta \mathrm{sgn}(k - 3k_F)$. In Fig. 3, the spin-correlation function $S(k)$ is plotted. Just like $S(k)$ from the exact solution,[2,3] the singularity at $2k_F$ is clearly demonstrated. Since $S_{2k_F}$ is finite, the power of $S(k)$ at point $2k_F$ requires a careful analysis. Using the form $\langle s_i^z s_j^z \rangle \sim |i-j|^{-\gamma} \cos(2k_F|i-j|)$ suggested by many authors,[3–6] one finds for $k = 2k_F + \Delta$:

$$S(k) - S_{2k_F} = \int_0^L dr \ (1 - e^{i\Delta r}) r^{-\gamma}$$

and

$$\frac{d[S(k) - S_{2k_F}]}{d\Delta} \sim \int_0^L dr \ e^{i\Delta r} \ r^{1-\gamma} \sim \frac{1}{\Delta^{2-\gamma}}.$$

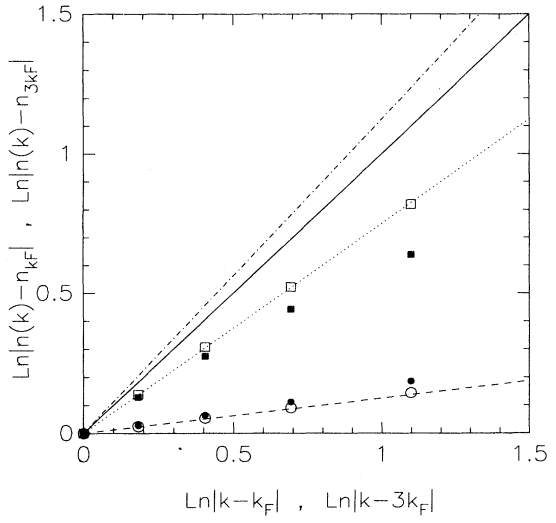


FIG. 4. The singularities of $n(k)$ at $k_F$ and $3k_F$ are displayed in this ln-ln plot. The data points plotted are for system size $L$ at the $k$ value that is the closest to $k_F$ or $3k_F$ for that $L$. The lines are of slope 1/8 (dashed), 3/4 (dotted), 1 (full line), and 9/8 (dot-dashed). The open circles are for $k < k_F$, and round dots are for $k > k_F$, while the open squares are for $k < 3k_F$, and black squares are for $k > 3k_F$.

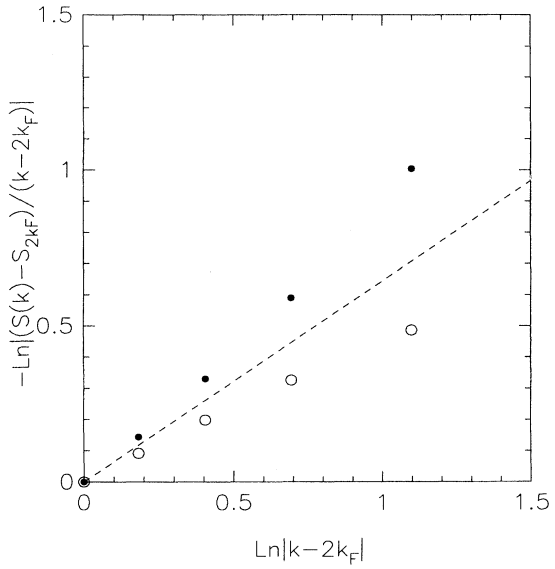


FIG. 5. The ln-ln plot of $[S(k) - S(2k_F)]/(k - 2k_F)$ around the singularity at $2k_F$. The dashed line is of power $-0.64$. The open circles are for $k < 2k_F$, and round dots are for $k > 2k_F$.

In Fig. 5, we have plotted $\ln[|S(k) - S_{2k_F}|/|k - 2k_F|] - \ln[|S(k_0) - S_{2k_F}|/|k_0 - 2k_F|]$ versus $\ln(|k - 2k_F|) - \ln(|k_0 - 2k_F|)$ for $k$, the closest but not equal to $2k_F$ at each $L$ with $k_0$ being the one for $L = 24$. We get $\gamma' \sim 0.64$ in $d[S(2k_F + \Delta) - S_{2k_F}]/d\Delta = C|\Delta|^{-\gamma'}$, where the power $\gamma$ in the coordinate representation $\langle s_i^z s_j^z \rangle \sim |i-j|^{-\gamma} \cos(2k_F|i-j|)$ is given by $\gamma = 2 - \gamma' \sim 1.36$. In order to investigate the effects of state truncation on the accuracy of our calculation, we have also calculated the exponents by keeping a smaller number of states $m = 80$. Comparing them with the results for $m = 100$, the values used for Fig. 4 and Table I, there is a typical change of about 1% for $L = 20$ and much less for smaller $L$. We have obtained essentially the same exponents using the $m = 80$ data. The resulting absolute error is larger for both $\alpha$ and $\beta$ for $m = 80$ than for $m = 100$, but relatively $\alpha$ deviates from 1/8 more than $\beta$ deviates from 3/4.

Taking into account the relative error $10^{-3}$ of $n(k)$ and the exponent deviation on both $k > k_F$ and $k < k_F$ sides, we get the range for the exponent $\alpha$, $0.08 < \alpha < 0.16$. Similarly, the range of the exponent $\beta$ is $0.7 < \beta < 0.8$. Both exponents $\alpha$ and $\beta$ are extracted from the $n(k)$ in the same way as discussed above. Since the relative error in $n(k)$ in both cases is about the same, the absolute error for both $\alpha$ and $\beta$ should be similar. For the power $\gamma$, we have not estimated its error since the data on both $k > 2k_F$ and $k < 2k_F$ sides are not good enough. From Fig. 5, it is clear that one needs a longer chain length to fix the power $\gamma$. The analytical results for the momentum-distribution function exponent at $k = k_F$ and the power-law decay of spin-spin correlation function are $\alpha = 1/8$ and $\gamma = 3/2$. Our calculations agree with these results. However, our calculated exponent $\beta$ at $k = 3k_F$ is 3/4, which is smaller than the analytical result $\beta = 9/8$. It is interesting to note that the calculated value is less than 1,

which makes the $3k_F$ singularity of the first order (i.e., the first derivative diverges, just like the one at $k_F$) instead of second order.

It is at present not clear what this discrepancy is due to. In our numerical simulations the chain length used may not be long enough. However, the exponent we calculated at $k_F$ is correct for the same chain length. On the other hand, the linear energy dispersion near the Fermi surface is an essential assumption in both bosonization and CFT treatments. Under this assumption the scaling relations between critical expoenents, i.e., only three of them are independent, have been derived.[3–6,15] These relations have been verified, to our knowledge, only for exponents near $k_F$ and $2k_F$.[3] As pointed out by Haldane,[7] and reemphasized recently by Schulz,[5] the deviation from linear dispersion in actual lattice models should give rise to high harmonics $q=(2n+1)k_F$, for any integer $n$, in the fermion operator expansion. This, in turn, may modify the exponents at $3k_F$. If, indeed, this is the case, our numerical results indicate that there is some unforseen physics to be explored. Another possibility is that the quarter filling is a special case, when higher harmonics intervene in numerics. Anyway, some further studies are certainly needed to clarify the issue.

We now discuss some technical aspects that enable us to calculate the correlation functions accurately using the DMRG method. We find that at each DMRG step, the algorithm with $m$ states being kept converges especially fast to the correct value at infinite $m$ at commensurate filling for the added block. For example, when studying quarter filling, we insert two sites at a time instead of one site, as normally done. The quarter filling is commensurate with adding one electron for two sites. We find that the convergence to the infinite $m$ value is much faster than at 3/8 filling, which is not commensurate, although in both cases the error as indicated by the weight of the retained states is quite similar. The latter point is understandable because the weight of retained states does not have an absolute meaning.[16] The reason for this superconvergence at the commensurate filling is because the DMRG is a real space technique. We need to keep states with different particle and spin ($S_z$) quantum numbers. When the particle density of the added block for the integer number of added electrons is exactly the same as the average density and when the density is uniform, the weight of the block states peaks at a particular value of particle and spin quantum numbers. It is then particularly efficient to save these states because the number of states for other quantum numbers nearby needed to be saved, is less. In order to keep the density uniform, we should use PBC. For the open boundaries the density is not uniform, and the superconvergence is lost. In addition, the PBC restores the translational invariance, which reduces the finite size effect and is essential for our calculation.

In summary, we have calculated the correlation functions in the strong coupling 1D Hubbard model using the finite chain DMRG method with PBC. We have calculated the spin correlation with its power law singularity at $k=2k_F$, and the momentum distribution with its critical exponents at $k=k_F$ and $k=3k_F$ for large $U$ ($U/t=10^3$). The calculated power for spin correlation at $k=2k_F$ and the exponent for momentum distribution at $k=k_F$ agree with the results of analytical analysis. However, the calculated exponent for momentum distribution at $k=3k_F$ is less than 1, and this result disagrees with the analytic prediction of 9/8. This problem should be investigated further since some unforseen physics may be involved.

One of the authors (S.Q.) wishes to thank Professor C. L. Wang, Dr. Hanbin Pang, Dr. Qinfeng Zhong, and Dr. Tiezheng Qian for various help and useful discussions. This work was partially supported by NSFC, LSEC, and CCAST. S.L. is supported by the Office of Naval Research Contracts Nos. N00014-92-J-1340 and N00014-95-1-0398 and by the National Science Foundation Grant No. DMR-9403201.

[1] P.W. Anderson and Y. Ren, in *High Temperature Superconductivity*, edited by K.S. Bedell *et al.* (Addison-Wesley, Reading, MA, 1989).

[2] E.H. Lieb and F.Y. Wu, Phys. Rev. Lett. **20**, 1445 (1968).

[3] M. Ogata and H. Shiba, Phys. Rev. B **41**, 2326 (1990); H. Shiba and M. Ogata, Int. J. Mod. Phys. B **5**, 31 (1991); M. Ogata, T. Sugiyama, and H. Shiba, Phys. Rev. B **43**, 8401 (1991); H. Shiba and M. Ogata, Prog. Theor. Phys. (Suppl.) **108**, 265 (1992).

[4] A Parola and S. Sorella, Phys. Rev. Lett. **64**, 1831 (1990).

[5] H.J. Schulz, Phys. Rev. Lett. **64**, 2831 (1990); Y. Ren and P.W. Anderson, Phys. Rev. B **48**, 16 662 (1993).

[6] H. Frahm and V.E. Korepin, Phys. Rev. B **42**, 10 553 (1990); **43**, 5633 (1991); N. Kawakami and S.K. Yang, Phys. Lett. A **148**, 359 (1990); J. Phys. Condens. Matter **3**, 5983 (1991); Prog. Theor. Phys. (Suppl.) **107**, 59 (1992).

[7] F.D.M. Haldane, Phys. Rev. Lett. **45**, 1358 (1980); Phys. Lett. **81A**, 153 (1981); Phys. Rev. Lett. **47**, 1840 (1981).

[8] Z.Y. Weng, D.N. Sheng, C.S. Ting, and Z.B. Su, Phys. Rev. Lett. **67**, 3318 (1991); Phys. Rev. B **45**, 7850 (1992).

[9] S. Sorella, A. Parola, M. Parrinello, and E. Tosatti, Europhys. Lett. **12**, 721 (1990).

[10] Except for the mention in Ref. 3 that this exponent is around 1 in the absence of a magnetic field, while it is bigger than 9/8 for one spin orientation and smaller for another in the presence of magnetic field.

[11] S.R. White, Phys. Rev. Lett. **69**, 2863 (1992); Phys. Rev. B **48**, 10 345 (1993).

[12] S.R. White and D.A. Huse, Phys. Rev. B **48**, 3844 (1993).

[13] E.S. Sorensen and I Affleck, Phys. Rev. Lett. **71**, 1633 (1993).

[14] Clare C. Yu and S.R. White, Phys. Rev. Lett. **70**, 3866 (1993).

[15] J. Solyom, Adv. Phys. **28**, 201 (1979).

[16] S. Liang and H. Pang, Phys. Rev. B **49**, 9214 (1994).